

On connecting the dynamics of the chromosphere and transition region with Hinode SOT and EIS.

Viggo H. HANSTEEN^{1,2} Bart DE PONTIEU² Mats CARLSSON¹ Scott MCINTOSH^{3,4}

Viggo.Hansteen@astro.uio.no

Tetsuya WATANABE⁵ Harry WARREN⁶ Louise HARRA⁷ Hirohisa HARA⁵

Theodore D. TARBELL² Dick SHINE² Alan TITLE² Carolus J. SCHRIJVER²

Saku TSUNETA⁵ Yukio KATSUKAWA⁵ Kiyoshi ICHIMOTO⁵ Yoshinori SUEMATSU⁵ Toshifumi SHIMIZU⁸

¹*Institute of Theoretical Astrophysics, University of Oslo, PB 1029 Blindern, 0315 Oslo Norway*

²*Lockheed Martin Solar and Astrophysics Laboratory, Palo Alto, CA 94304, USA*

³*Department of Space Studies, Southwest Research Institute, 1050 Walnut St, Suite 400, Boulder, CO 80302, USA*

⁴*High Altitude Observatory, National Center for Atmospheric Research, PO Box 3000, Boulder, CO 80307, USA*

⁵*National Astronomical Observatory of Japan, Mitaka, Tokyo, 181-8588, Japan*

⁶*Space Science Division, Naval Research Laboratory, Washington DC, USA*

⁷*Mullard Space Science Laboratory, University College London, UK*

⁸*ISAS/JAXA, Sagami-hara, Kanagawa, 229-8510, Japan*

(Received 2000 December 31; accepted 2001 January 1)

Abstract

We use coordinated Hinode SOT/EIS observations that include high-resolution magnetograms, chromospheric and TR imaging and TR/coronal spectra in a first test to study how the dynamics of the TR are driven by the highly dynamic photospheric magnetic fields and the ubiquitous chromospheric waves. Initial analysis shows that these connections are quite subtle and require a combination of techniques including magnetic field extrapolations, frequency-filtered time-series and comparisons with synthetic chromospheric and TR images from advanced 3D numerical simulations. As a first result, we find signatures of magnetic flux emergence as well as 3 and 5 mHz wave power above regions of enhanced photospheric magnetic field in both chromospheric, transition region and coronal emission.

Key words: Sun: chromosphere – Sun: transition region – Sun: corona – Sun: UV radiation – Sun: flux emergence

1. Introduction

The Hinode spacecraft, launched in late September 2006, is comprised of three scientific instruments (Kosugi et al. 2007): the Solar Optical Telescope (SOT), the Extreme ultraviolet Imaging Spectrograph (EIS), and the X-Ray Telescope (XRT). The SOT is designed to produce high quality images and measurements of the magnetic field in various photospheric and chromospheric lines and continua (Tsuneta et al. 2007). The ultraviolet and X-ray instruments are constructed to extract information from the outer solar atmosphere. In particular, EIS (Culhane et al. 2007) observes in two bands (180 – 205 Å and 250 – 290 Å) that feature a number of coronal and some transition region emission lines.

An explicitly stated primary scientific goal of the Hinode mission is to map and understand the transport of mechanical energy flux between the lower lying layers of the Sun's atmosphere and the corona, as well as the relation between the structure of the photospheric magnetic field and coronal heating. Generally speaking there are two ways of transporting energy from the convection zone and into the layers above: either by utilizing waves, such as the 5-minute p-modes or chromospheric 3-minute oscillations, or by converting the energy contained in the mag-

netic field, stressed by photospheric flows and granular evolution, in some episodic fashion into heat in the chromosphere and/or corona. Related questions are what role magnetic flux emergence plays in injecting energy into the chromosphere/corona and replenishing the previously existing field; and with what efficiency acoustic and Alfvén waves are generated and propagated through the chromosphere and transition region. In this paper we report on preliminary simultaneous observations made with the SOT and EIS instruments to shed light on these issues.

2. Instrumental setup and Observations

During a two-week period in February 2007 we observed several types of solar region including coronal hole, quiet Sun, network, and plage/small active regions both on the disk and towards the solar limb. A substantial amount of time was spent following the progress of the small active region NOAA 10942 as it transverses the disk from a solar position of roughly –400 arcsec to the west of disk center on February 20 to a position of 900 arcsec east, near the eastern limb on February 27.

With SOT we obtained magnetograms measured in the Fe I 630.2 nm line and Ca II 396.8 nm H-line images at high (4–11 s cadence) for the observations described here. The

Ca II H-line filter used with SOT is fairly wide (0.22 nm) and thus includes a significant fraction of line wing in addition to line core. We have collected similar image series in the G-band and in the blue continuum channel of SOT's broad band filtergraph but those observations are not described here.

The EIS instrument also supports a number of observing modes. We report on observations made with the 40 arcsec wide slot that forms a 40 arcsec wide image of the Sun in particular (strong) emission lines on the detector. This observing mode has the advantage of allowing images to be recorded at relatively high cadence (30 s or so for the strongest lines), but incurs the cost of removing any easily derived velocity or line-width signal as well as a slightly worse spatial resolution than that achieved with the 1 arcsec slit. We also report on raster observations made by stepping the 1 arcsec slit in 1 arcsec increments across the region of interest. With exposure times of 30-60 s a typical raster takes of order an hour to complete. The spectral resolution of EIS is 0.00223 nm; roughly 27 km/s at 25.0 nm or 35 km/s at 19.0 nm. We have also collected several sit-and-stare time series with an immobile 1 arcsec slit, but will present results from these at a later date.

In normal operation the Hinode spacecraft tracks a given solar feature, correcting for solar rotation. In principle, co-alignment between data sets obtained by the various instruments becomes a question of finding the offsets between the instruments and applying these to the collected data. After the EIS coarse mirror move of January 24 2007, the EIS offset is some 3 arcsec east and 50 arcsec south of the center of the SOT field of view. In actual practice finding the correct offsets is not always straightforward. As will be emphasized in this paper it is sometimes far from simple to identify corresponding solar features at photospheric/lower chromospheric heights with those found in the transition region and corona, especially considering the mismatch in spatial resolution between the SOT and EIS instruments. When in serious doubt about alignment we found it helpful to co-align via TRACE observations by identifying features found in TRACE Fe IX/x 17.1 nm and EIS Fe XII, as well as the TRACE 160.0 nm channel and the SOT Ca H-line.

It must also be borne in mind that SOT has a correlation tracker that removes most of the orbital variations on SOT pointing while EIS does not have such a device: Flexing due to temperature variations of the EIS instrument during an orbit can be as large as 5 arcsec in the north/south direction and 2–3 arcsec in the east/west direction. We have removed some of this variation by internally co-aligning the images in EIS time-series. We believe we have achieved a co-alignment that is generally better than 2 arcsec.

3. Results

3.1. Quiet Sun with weak plage

On February 19 2007, from roughly 11:30 to 17:30 we observed a quiet Sun region that also contained weak plage

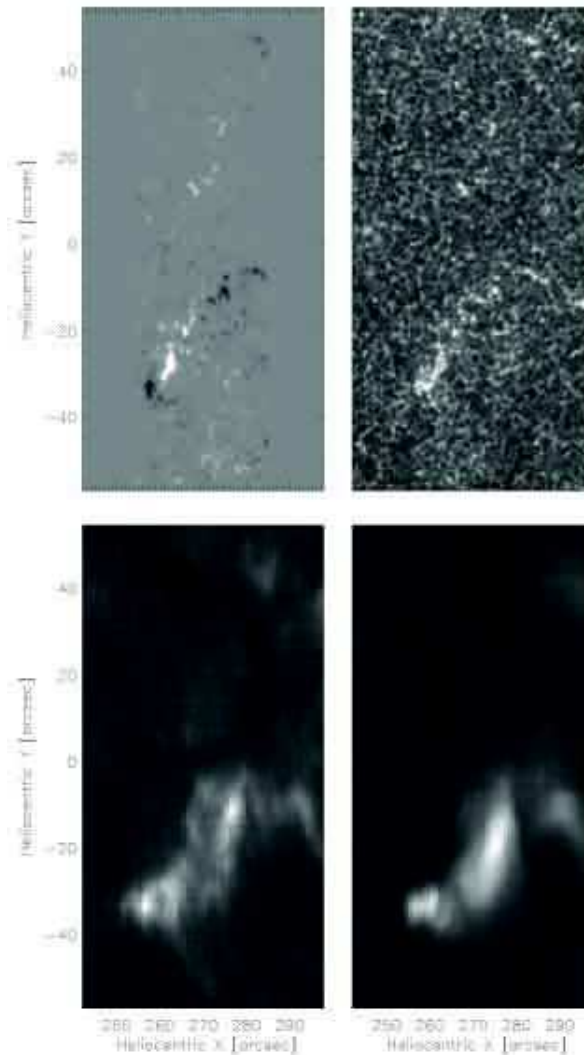


Fig. 1. Co-pointed SOT and EIS images of a quiet Sun region centered on heliocentric co-ordinates (280,0) arcsec obtained February 19, 2007. In the upper left panel we show a Fe I 630.2 nm magnetogram and in the upper right panel the Ca II 396.8 nm H-line. In the lower panels the corresponding EIS raster images for the transition region He II 25.6 nm (left) and the coronal Fe XII 19.5 nm (right) lines are shown.

of both polarities. In Figure 1 we show co-pointed individual frames from the SOT and EIS rasters that zoom in on the region observed with the SOT.

In the upper left panel we show an image from the SOT magnetogram movie. The field consists of several small magnetic elements of both polarities spread across the image. In addition, we find a stronger plage region stretching from (255,-35) to (280,-5) in heliocentric coordinates. There is also some weaker plage centered at (270,15) and (283,45). In the movie the magnetic field, churned by the motions of the photosphere, shows motions of the individual flux elements that presumably correspond to G-point bright points as well as the bright points seen in the Ca II H-line images. Flux elements of opposite polarity some-

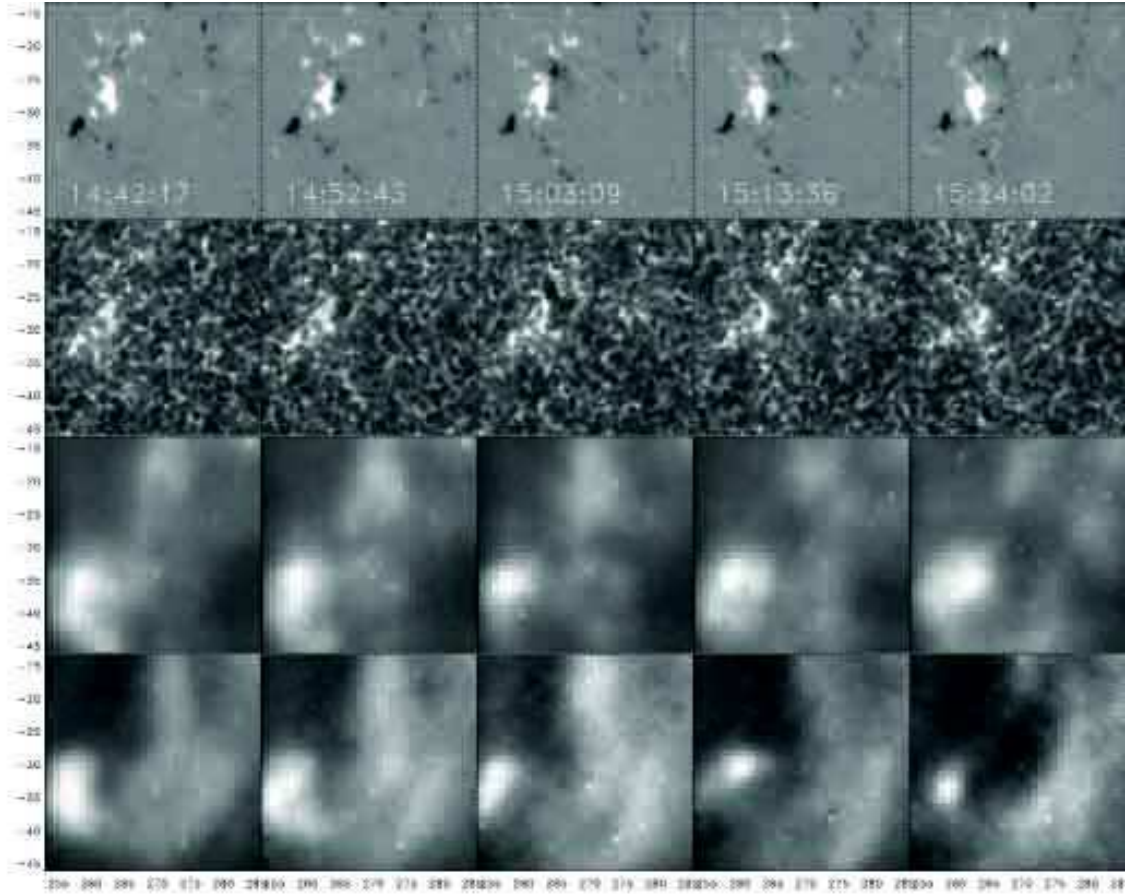


Fig. 2. Co-pointed SOT and EIS images of a quiet Sun region centered on heliocentric co-ordinates (280,0) arcsec obtained February 19, 2007. This set of images shows the time evolution of a cutout of the region shown in Figure 1 that illustrates the flux emergence that occurs from roughly 14:45 UT to 15:30 UT (at which time the EIS time series completed). The top panels show Fe I 630.2 nm magnetograms separated by some 10 minute intervals. The three following rows of panels show the chromospheric Ca II 396.8 nm H-line, the transition region He II 25.6 nm line and the coronal Fe XII 19.5 nm line at the same instants in time.

times meet and merge, disappearing from view, at other times flux elements appear and move apart. In the weak plage regions of greater magnetic field concentration the field seems less responsive to photospheric motions, or alternately photospheric motions are suppressed by the presence of the field. The general topology of the plage is unchanged during the six hours this region of the Sun was observed. We did however, observe an incidence of flux emergence in the central portion of the plage region; negative (black) field appears at (265,-25) just to the right of the large collection of positive (white) field present in figure 1, rapidly splitting in two with one collection of field moving northeast and the other more or less staying in place. This new flux is largely dissipated at the end of the time-series roughly one hour after it first appears. Detailed images of the time evolution of the flux emergence are shown in Figure 2.

The magnetic topology outlined by the small plage region is evident in all three of the wavelength bands shown in Figure 1.

The Ca 396.8 nm H-line, shown in the upper right panel of Figure 1, is formed partly in the photosphere, partly in

the chromosphere (Carlsson et al. 2007). Clearly visible throughout the image is the reverse granulation formed just above the visible photosphere. Movies made of the Ca H-line show the expected evolution of the reverse granulation as well as the fairly large scale intensity variations due to photospheric p-modes and chromospheric 3-minute oscillations. Also spread throughout the image are bright points, corresponding to G-band bright points where one can see deeper into the solar atmosphere. The bright points associated with the small magnetic field elements and the plage show motions well correlated with the motions of the underlying field. In addition, especially surrounding the plage, we find ‘hazy’ regions that most likely image chromospheric emission at heights far above the photosphere: movies constructed using a high-pass frequency filter (retaining only frequencies > 25 mHz) show that this haze corresponds to the ‘straws’ seen with 0.1 nm wide Ca H-line filtergram movies at the Dutch Open Telescope (Rutten 2007) and on the solar limb with Hinode (De Pontieu et al. 2007). (Straws appear hazy since they are nearly straight, short-lived features that are formed at middle to upper chromospheric heights, and

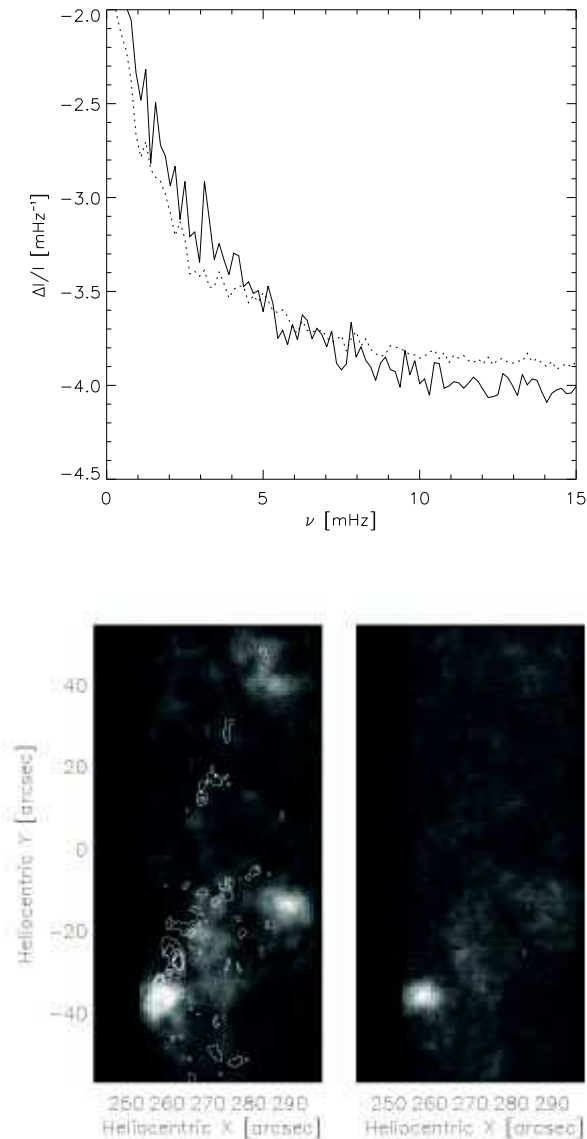


Fig. 3. The upper panel shows the power frequency spectrum for the variation of the logarithm of the intensity $\Delta I/I$ for the He II 25.6 nm line in the February 19, 2007 quiet Sun data-set for a subset of the brighter pixels found in the vicinity of the weak plage region (solid line) and for a subset of pixels imaging typical quiet Sun regions (dotted line). The lower panels show maps of the location of power in this line in 1 mHz wide bands centered on 3 mHz (left panel) and 5 mHz (right panel). Overplotted on the 3 mHz map are the contours of the SOT magnetogram shown in Figure 1. Axes are heliocentric co-ordinates measured in arcseconds.

that are weak because of the large photospheric contribution to the wide Ca H filter used on SOT.)

As seen in Figure 2 the region co-spatial with and/or just above the region of flux emergence seen in the magnetogram movies initially shows a dimming in the Ca H-line filtergrams. Flux is first seen to emerge in the magne-

tograms at 14:44 UT. This is followed by what appear to be two to three large dark granules in the Ca-H-line some 10 minutes later at 14:55 UT. These dark granules expand and move with the emergence of the field. The border of this dark region becomes filled with bright points within 20 minutes of the fields emergence. As time passes the dark granules brighten, seemingly as a result of ‘haze’ filling in the dark region, which upon inspection of difference and high-pass frequency filtered movies are revealed to consist of loop-like structures in the Ca-H-line that join the newly formed bright points.

In the lower left panel of Figure 1 we show a raster image of the He II 25.6 nm line which is formed in the 80,000 K transition region, in the lower right panel we show the Fe XII 19.5 nm coronal line which is formed at some 1 MK. In both lines we see the weak plage region, stretching from (255,-35) to (280,-5), delineated quite clearly. This is also true for some of the smaller and weaker plage regions to the north. On the other hand, the correspondence between bright emission as seen in the transition region and coronal lines and magnetic flux measured in the photosphere does not extend all the way down to magnetic structures of the smallest spatial scales. This lack of correspondence has been observed previously in moss regions on spatial scales of 1 arcsec (de Pontieu et al. 1999).

EIS 40 arcsec slot images of a number of strong lines, including the He II and Fe XII lines were observed contemporally with the SOT movies described above. These slot movies show large temporal variations at cadences down to those measurable by the 30 s exposure time; the general topology outlined by the plage region is maintained, also in the upper solar atmosphere, but the emission is strongly variable at any given location both within the plage and outside in the weaker field quiet Sun. These variations do not show an obvious one-to-one correspondence with events that are transpiring below: Some of the magnetic flux cancellations as two opposite polarity elements coalesce are accompanied by brightening in the He and Fe lines and some are not. The 3/5 minute wave pattern that is clearly discernible in the Ca H-line emission does not leave an obvious footprint in the lines formed above. An exception to this rule of non-correspondence is the large flux emergence event that happens in the plage. As is clear by inspection of Figure 2 both the He II and the Fe XII lines show an dimming dark “bubble” that appears at 15:14 UT and expands thereafter, almost 30 minutes after the flux emergence is obvious in the magnetograms. Unfortunately, we did not observe the end of this event with EIS as another observing program was started at 15:30 UT.

3.2. Wave Propagation

While there were few obvious correlations between the movies made with SOT filtergrams and the EIS slot, an initial insight into the role of waves can be found by considering the power contained in the 3- and 5-minute frequency bands of this region in EIS He II slot movies. In the upper panel of figure 3 we show the computed power spectra of the variation of the intensity $\Delta I/I$ for a subset

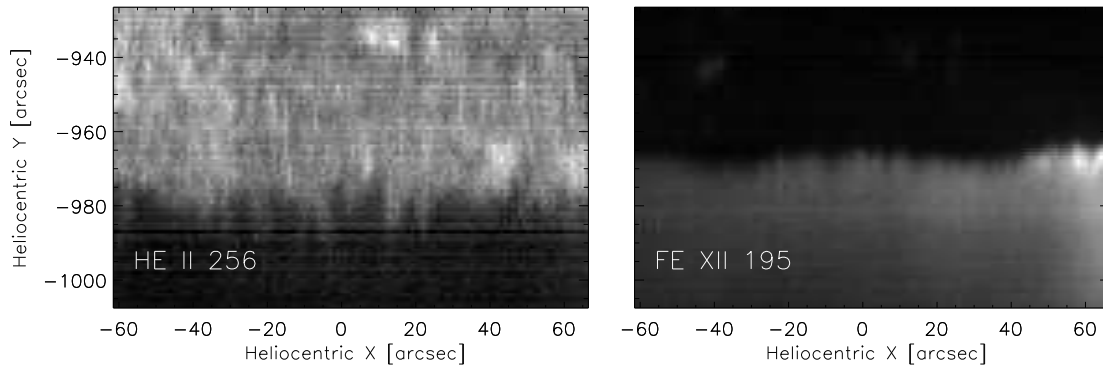


Fig. 5. South limb images made from rasters in the He II 25.6 nm and Fe XII 19.5 nm lines obtained February 16, 2007. Note the (macro)-spicules in the He II line and that similar features appear in absorption in the Fe XII line. Axes are heliocentric co-ordinates measured in arcseconds.

of the brighter pixels found in the vicinity of the plage region (solid line) and for a subset of pixels imaging typical quiet Sun regions (dotted line). The spectra show some excess power for the brighter region, in both 3 and 5 minute bands, while the power found in the quiet Sun region is of questionable significance. Note however, that the wave power found in the transition region is known from SUMER observations (*e.g.* McIntosh et al. 2001) to be quite dependent on the topology of the magnetic field in the chromosphere below. Significant 5 minute power in coronal lines has been observed before with TRACE, *e.g.*, in the TRACE 17.1 nm and 19.5 nm bands in loops (de Moortel et al. 2002a; de Moortel et al. 2002b) as well as in the moss (De Pontieu et al. 2003; De Pontieu et al. 2005). Likewise, 3 minute power in coronal emission above active regions has also been seen before Brynildsen et al. (2000) in the TRACE 17.1 nm band.

Maps of the location of the Fourier power of the intensity variation $\Delta I/I$ of the He II 25.6 nm line were constructed by taking the sum over time of the absolute value of the Fourier filtered intensity signal. In the lower panels of Figure 3 we show the power maps derived for 1 mHz wide bands centered on 3 mHz (left panel) and 5 mHz (right panel). We find the power to be concentrated in the vicinity of the plage as indicated by the contours of the absolute value of the magnetic field strength drawn into the 3 mHz map. This could be an example of the leakage of p-modes into the upper atmosphere along inclined magnetic field lines (*e.g.* De Pontieu et al. 2004). However, identification of these intensity variations as wave-like as opposed to being a result of evolution (of *e.g.* the magnetic field) awaits the analysis of EIS velocities in sit-and-stare studies with sufficiently high cadence. Future work involving field extrapolations based on the SOT magnetograms and travel time analysis in the lower atmosphere will also be necessary to confirm this and/or to pin down the exact leakage mechanism.

3.3. Transition region velocity events

While our slot movies and intensity raster maps do not show any clear evidence of small scale features that can be linked with the lower atmosphere, velocity maps made in the transition region He II 25.6 nm line do show small scale structure that should have some lower lying counterpart. In the lower panels of Figure 4 we present velocity maps of the rasters obtained in the vicinity of the small active region NOAA 10942.

The velocity maps are both normalized so as to show line shifts of ± 25 km/s relative to the average line shift, with black color indicating upward blue-shifts and white indicating down-flowing red-shifts. The velocities show a fairly complex structure, and quite striking are the numerous intense (> 25 km/s) blue-shifts found throughout the quiet Sun region of the images. (This type of event is found in every raster made in the He II line that includes quiet Sun emission during the two-week period covered by this study). Note that the blue-shifts are not evident in the 1 MK plasma imaged by the Fe XII line shown in the lower right panel. The linear extent of these phenomena is less than 1 arcsec^2 . Note that that the S x blend known to be located near the He II line is on the *red* side of the He II line (and is visible to the red of the He II line in spectra taken above the limb).

The line profile of a typical up-flow event (solid line) along with the average line profile in the He II 25.6 nm line is shown in the upper panel of Figure 4. The actual velocity in the up-flow event is larger than the average velocity derived by taking the first moment of the line: the upper panel line profile reveals that the line is split into two components, the component found in the blue wing has a relative shift of some 100 km/s. This phenomena may be similar to the events found by Dere et al. (1984) with the HRTS instrument.

We are currently examining the SOT magnetograms

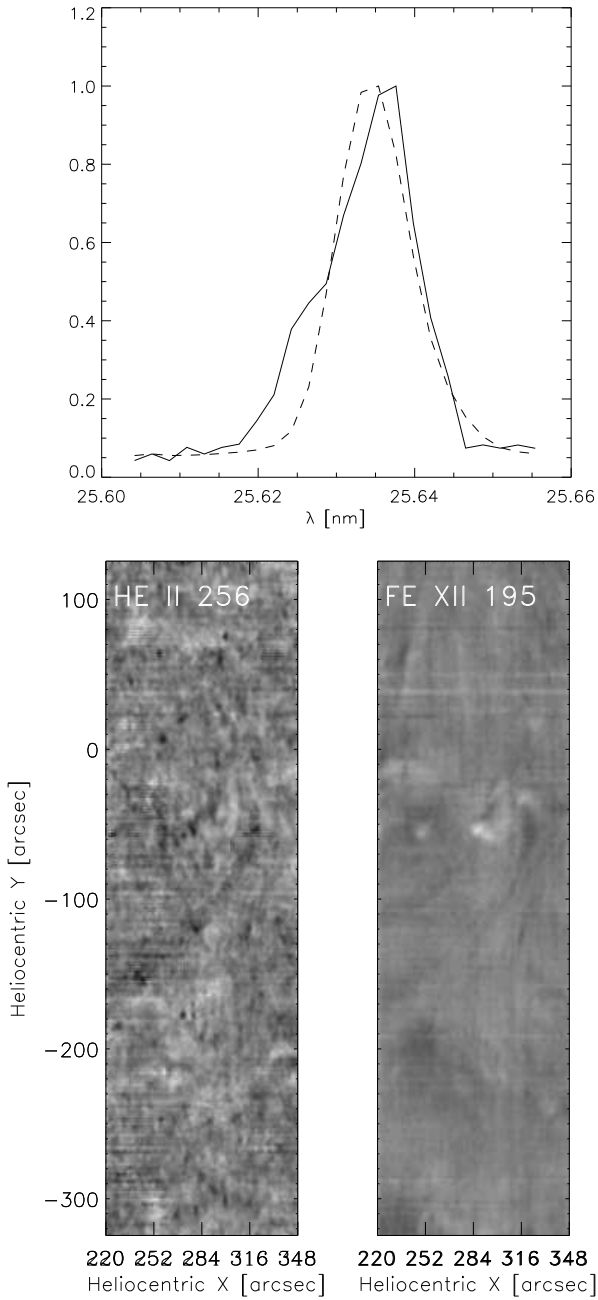


Fig. 4. The upper panel shows line profiles of the He II 25.6 nm line: Average line profile (dashed line) and a profile showing high velocity event (solid line), as described in the text, and shown in the velocity maps in the lower panels, where the high velocity events are evident as small dark dots in the image. The right panel shows a velocity map of the Fe XII 19.5 nm line. The velocity maps were made from rasters obtained on February 19, 2007 and have a range of ± 25 km/s. Axes are heliocentric co-ordinates measured in arcseconds.

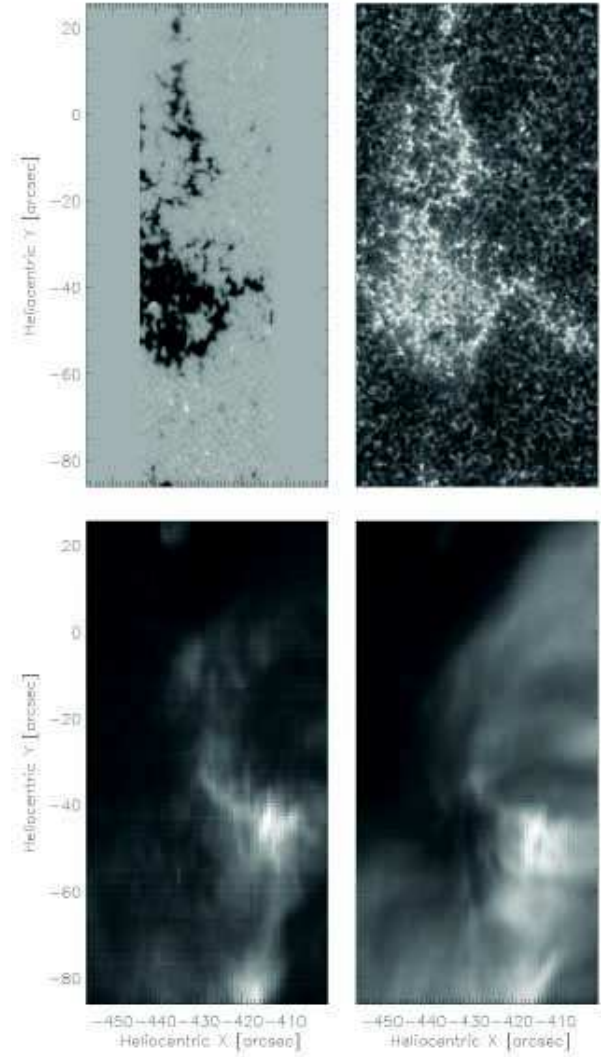


Fig. 6. Co-pointed SOT and EIS images of the small active region NOAA 10942 centered on solar co-ordinates (-430,-30) obtained February 20, 2007. In the upper left panel we show a Fe I 630.2 nm magnetogram and in the upper right panel the Ca II 396.8 nm H-line. In the lower panels the corresponding EIS raster images for the transition region He II 25.6 nm (left) and the coronal Fe XII 19.5 nm (right) lines are shown. Axes are heliocentric co-ordinates measured in arcseconds.

to see whether we can find any correlations between the merging or appearance of magnetic elements and these up-flow events seen in He II, but our first impression is that there is no one-to-one correspondence between these events.

3.3.1. Spicules and macro-spicules

As an aside, we mention the possibility that there is a connection between the up-flow events described here and the He II (macro)-spicules observed above the limb. An example is the EIS raster made on the southern pole limb on February 16 2007, shown in Figure 5. Similar spicules have been observed previously in the EUV passband by SOHO/SUMER (Wilhelm 2000). The observed “spicules” appear as largely radial features extending some 10 arcsec above the limb with widths of order 1 – 2 arcsec (*i.e.* roughly the resolution of EIS). The spicules show up in *absorption* in the Fe XII line: The bulk of the plasma in this phenomena seems not to be heated to coronal temperatures. Note that the spicules are quite numerous, they are also continually present in slot movies made on the same date, but the lower resolution of the slot mode hinders accurate identification and the measurement of lifetimes, birthrates or other properties, nor indeed correlation with the Ca H-line spicules found above the limb.

3.4. NOAA 10942

The difficulties in connecting phenomena in the lower solar atmosphere with the transition region and corona is driven home by the extended set observations made of NOAA 10942 made on February 20 (and every day thereafter until February 27). In the photosphere this region displays a large aggregate of (largely) unipolar field as shown in the upper left panel of Figure 6. The Ca H-line images, upper right panel, show enhanced emission in the plage region, presumably both from the photosphere and from the chromosphere above. A small pore is apparent towards the lower part of the plage.

It is very difficult to pick out the structure of the plage region in images taken of the hotter plasma above, as should be clear from the He II 25.6 nm and Fe XII 19.5 nm images shown in the lower panels of Figure 6 as well as from the larger field of view images shown in Figure 7. The brighter regions in the transition region and coronal lines lie somewhat to the east of the plage region and most of the hotter loops seen in Fe XII extend eastward, apparently rooted in the western edge of the plage region. Note that also all the rasters made with the EIS instrument, including those shown in Figure 7 differ markedly from each other. The He II emission seems to mainly consist of shorter loops and perhaps hints of chromospheric network (though the correlation with the Ca H-line emission is poor in this example). The Si VII 27.5 nm line, formed in the upper transition region at 630 kK, shows emission in the plage region offset slightly to the west compared to He II and Fe XII. The loops in this line mainly extend north-westward across the plage, the eastward directed loops are partial, presumably footpoints of the hotter, eastward oriented, loops we find in Fe XII and in the Fe XV 28.4 nm line formed at some 2.1 MK.

4. Conclusions

Both differences in instrument temporal and spatial resolution as well as fundamental differences between the photosphere/chromosphere and the outer solar layers comprising the transition region and corona are significant stumbling blocks in understanding the coupling between these regions. Even though the Hinode spacecraft presents us with tools of unprecedented sophistication for unravelling the complex of physical processes that control the outer layers of the Sun, a successful result will require using advanced analysis techniques. It is fortunate that these techniques are entering the scene concurrently with the observations so as to make comparison between theory and observation meaningful.

Hinode is a Japanese mission developed and launched by ISAS/JAXA, collaborating with NAOJ as domestic partner, NASA and STFC (UK) as international partners. Scientific operation of the Hinode mission is conducted by the Hinode science team organized at ISAS/JAXA. This team mainly consists of scientists from institutes in the partner countries. Support for the post-launch operation is provided by JAXA and NAOJ (Japan), STFC (U.K.), NASA (U.S.A.), ESA, and NSC (Norway). This work was supported by the Norwegian Research Council grant 170926.

References

- Brynildsen N., Maltby P., Leifsen T., Kjeldseth-Moe O., Wilhelm K., Jan. 2000, *Sol. Phys.*, 191, 129
- Carlsson M., Hansteen V.H., De Pontieu B., et al., 2007, *PASJ*, in Press
- Culhane J.L., Harra L.K., James A.M., et al., Mar. 2007, *Sol. Phys.*, 60–+
- de Moortel I., Hood A.W., Ireland J., Walsh R.W., Sep. 2002a, *Sol. Phys.*, 209, 89
- de Moortel I., Ireland J., Walsh R.W., Hood A.W., Sep. 2002b, *Sol. Phys.*, 209, 61
- de Pontieu B., Berger T.E., Schrijver C.J., Title A.M., Dec. 1999, *Sol. Phys.*, 190, 419
- De Pontieu B., Erdélyi R., de Wijn A.G., Sep. 2003, *ApJL*, 595, L63
- De Pontieu B., Erdélyi R., James S.P., Jul. 2004, *Nature*, 430, 536
- De Pontieu B., Erdélyi R., De Moortel I., May 2005, *ApJL*, 624, L61
- De Pontieu B., McIntosh S., Carlsson M., et al., 2007, *Science*, submitted
- Dere K.P., Bartoe J.D.F., Brueckner G.E., Jun. 1984, *ApJ*, 281, 870
- Kosugi T., Matsuzaki K., Sakao T., et al., 2007, *Sol. Phys.*, in Press
- McIntosh S.W., Bogdan T.J., Cally P.S., et al., Feb. 2001, *ApJL*, 548, L237
- Rutten R.J., Mar. 2007, *ArXiv Astrophysics e-prints*
- Tsuneta S., Suematsu Y., Ichimoto K., et al., 2007, *Sol. Phys.*, submitted
- Wilhelm K., Aug. 2000, *A&A*, 360, 351

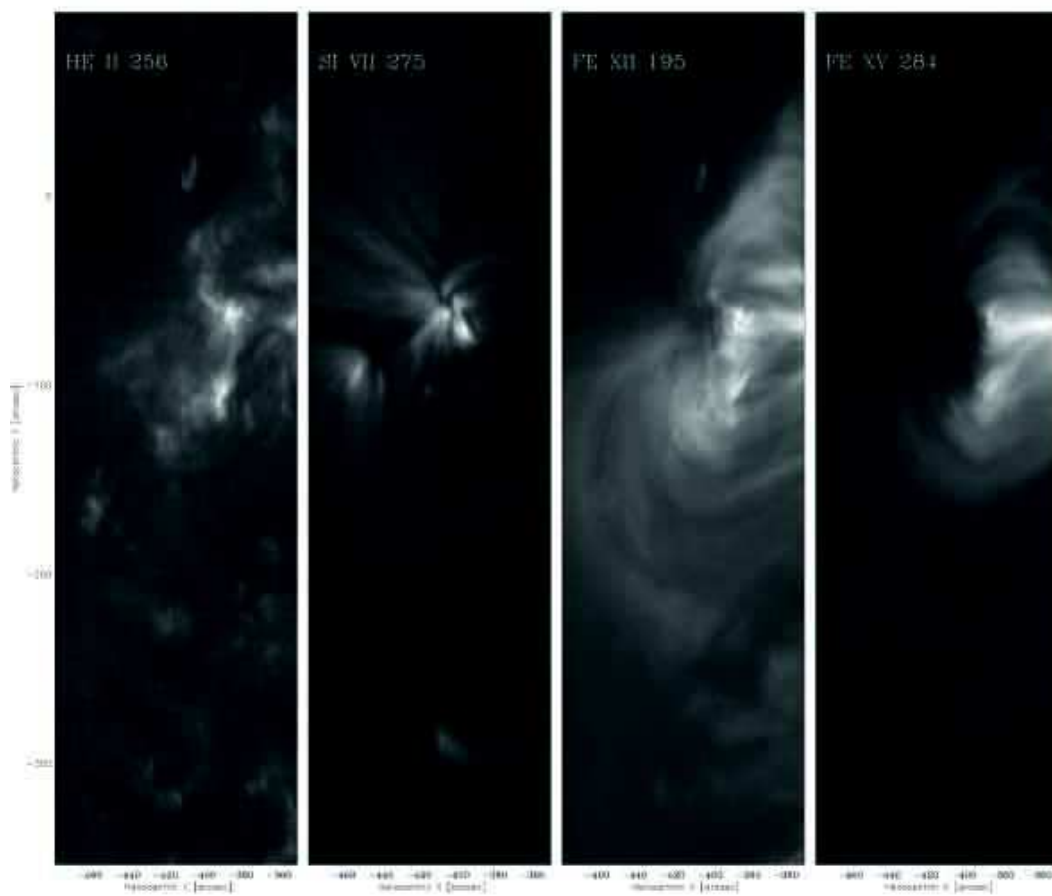


Fig. 7. Intensity maps of NOAA 10942 made from EIS rasters on February 20, 2007. From left to right the lines shown are He II 25.6 nm, Si VII 27.5 nm, Fe XII 19.5 nm and Fe XV 28.4 nm. Axes are heliocentric co-ordinates measured in arcseconds.